Available online at www.sciencedirect.com
ScienceDirect
Catalysis Today 116 (2006) 422–432
CATALYSIS TODAY
www.elsevier.com/locate/cattod

Methanol electrooxidation on PtRu nanoparticles supported on functionalised carbon black

J.L. Gómez de la Fuente [a], M.V. Martínez-Huerta [b,*], S. Rojas [a], P. Terreros [a], J.L.G. Fierro [a], M.A. Peña [a]

[a] *Instituto de Catálisis y Petroleoquímica, CSIC, Marie Curie 2, E-28049 Madrid, Spain*
[b] *Departamento de Química Física, Universidad de La Laguna, c/Astrofísico Francisco Sánchez s/n, E-38071 La Laguna, Tenerife, Spain*

Available online 10 July 2006

Abstract

The effect of the preparation method of PtRu electrocatalysts and the chemical treatment of support on the performance for methanol electrooxidation has been studied. Carbon supported PtRu catalysts were synthesized from aqueous solution of H_2PtCl_6 and $RuCl_3$ precursors by two different methods: colloidal (using $NaHSO_3$) and impregnation. The carbon black Vulcan XC-72R was functionalised with H_2O_2 and HNO_3. A commercial PtRu/C catalyst purchased from Johnson and Matthey was used as reference. The obtained electrocatalysts were characterized by XPS, XRD, TEM, EGA-MS, TGA and TXRF. Chronoamperometry in methanol and CO_{ads} stripping experiments were conducted to check their electrocatalytic activity. Electrocatalysts obtained by the colloidal method and supported on functionalised carbon black with HNO_3 and especially with H_2O_2, showed better performances (CO tolerance and superior methanol oxidation ability) than those obtained by the impregnation method and the commercial one.

Keywords: Pt–Ru catalysts; Direct methanol fuel cells; Carbon

1. Introduction

Methanol oxidation has been receiving great attention during last decades due to the possible application in direct methanol fuel cells (DMFC), which show great promise as high-efficiency, low-emission future power sources [1,2]. Considerable effort has been devoted to the technical realization of the methanol fuel cell, and mainly to develop highly active methanol electrooxidation catalysts. Electrochemical experiments have shown that CO, formic acid and formaldehyde are intermediates in the oxidation of methanol on a Pt electrode [3,4]. The direct reaction via adsorbed carbon monoxide, CO_{ad}, involves several dehydrogenation steps, which may occur via C-species bonded to the surface as suggested by Bagotski et al. [5]:

$$CH_3OH \rightarrow Pt{-}CH_2OH \rightarrow (Pt)_2{-}CHOH \rightarrow (Pt)_3{-}COH \rightarrow Pt{-}CO \rightarrow CO_2$$

This sequence of steps shows that several neighbouring Pt sites are necessary for the oxidation via CO_{ad}. CO is strongly adsorbed on the Pt surface reducing considerably its electroactivity. Accordingly, platinum metal alone could never be a good catalyst for continuous fuel cell operation at room temperature or even higher (e.g. 60 °C). However, no better catalyst than Pt, at least in acid medium, for breaking C–H and O–H bonds in methanol molecules is known at present. Therefore, methanol electrooxidation at reasonable rates in acid media is only conceivable on Pt-based catalysts. Nowadays, the state-of-the-art of these materials are PtRu electrocatalysts supported on carbon [6]. The oxidation of adsorbed CO is postulated to be the rate-determining step and Ru is widely accepted as a promoter for the CO oxidation, commonly explained on the basis of the bifunctional mechanism [7] or "ligand effect" [8] or a contribution of both. The bifunctional mechanism assumes that Ru promotes the oxidation of the strongly bound CO on Pt by supplying an oxygen source (Ru–OH_{ad}). According to the ligand effect, the energy level of the catalyst is changed so that the binding strength of adsorbed CO is weakened, thereby reducing the oxidation overpotential. However, improvement of effective electrocatalysts for the electrooxidation of methanol in acid solutions

* Corresponding author. Tel.: +34 91 585 4879; fax: +34 91 585 4760.
E-mail address: mmartinez@icp.csic.es (M.V. Martínez-Huerta).

0920-5861/$ – see front matter © 2006 Elsevier B.V. All rights reserved.
doi:10.1016/j.cattod.2006.05.083

is an essential goal in the development of a practical methanol fuel cell.

Carbon black is often employed as support for noble metals in the electrodes of solid polymer fuel cells. This support is of special interest due to the high surface area, that allows fine dispersion, stabilisation of small metallic particles and drastically reduce the metal loadings [9,10]. Vulcan XC-72 is the more frequently used carbon support for the preparation of DMFC catalysts. The main reason for this lies in the fact that Vulcan XC-72 exhibits a small amount of micropores and a reasonably high surface area sufficient to accommodate a high loading of the metal phase [6].

The impact of the chemical and physical properties of the carbon on the catalytic performance in the electrooxidation of methanol is not yet sufficiently understood. The presence of oxygen surface complexes influences the surface behaviour of carbons to a great extent [11]. As examples, the wettability and adsorptive behaviour of a carbon, as well as its catalytic and its electrical properties, are influenced by the nature and extent of the oxygen complexes. It is known that the surface of the carbon black can be modified by oxidation treatments, and several types of surface functional groups can be produced as a consequence of these treatments [12–14]. Thus, carboxylic, phenolic, carbonyls, anhydrides, lactones, peroxides and quinones have been suggested as acidic surface groups produced by oxidation treatments. Surface oxygen complexes of the support exhibit an outstanding role in this field due to their double function: (a) they are anchorage sites for the metal precursor during catalyst preparation, and (b) they can act as active centres in multifunctional catalysts due to their acid–base or redox properties. When the support is a hydrophobous material, like carbon, surface complexes also contribute to improve its wettability and hence make the impregnation with polar solvents easier. In liquid feed fuel cells it can be desirable to make components in the anode (e.g. catalyst layer) more wettable by liquid fuel stream in order to improve access of the reactant to the electrocatalyst sites [15].

The varying role of oxygenated functionalities on the formation of the dispersed platinum is well recognized [16–19]. However, conflicting points of view regarding the effect of the metal dispersion, the oxidation state of the metal and the nature of the metal–support interaction on the catalytic behaviour are found in the literature. Recently, Pt catalysts supported on electrochemically oxidized glassy carbon has been studied [20]. Electrochemical treatment of a glassy carbon support does not affect significantly the real Pt surface area but leads to a better distribution of platinum on the substrate and has remarkable increase in methanol oxidation, for more than one order of magnitude larger than Pt/glassy carbon electrode. The oxidation of the substrate by ozone treatment also affects the performance of PtRu/C [21]. Electrochemical measurements showed that the catalysts supported on the carbon after ozone treatment had higher activity for methanol electrooxidation than PtRu/C supported on the untreated carbon black.

This paper presents the results obtained in a study of the role of oxygenated surface groups of carbon supports on the Pt and Ru morphology electrocatalyst and their performance in the direct methanol fuel cells, maintaining constant other variable concerned with the metal loading and Pt/Ru ratio. As part of this study two different catalyst preparation methods were investigated.

2. Experimental

A commercial carbon black Vulcan XC-72R (Cabot) was used as a support. This carbon (labelled as Vulcan) was functionalised [16] with two different oxidizing reagents: (i) treatment with HNO_3 aqueous solution (10 wt.%) at room temperature during 48 h (sample labelled as Vulcan-N), and (ii) treatment with H_2O_2 (10%, v/v) at room temperature during 48 h (sample labelled as Vulcan-O). The functionalited HNO_3 and H_2O_2 carbons were dried at 120 °C during 24 h. The catalysts were prepared by two different methods:

2.1. Impregnation method

The supports Vulcan, Vulcan-N and Vulcan-O were impregnated at 80 °C with an aqueous solution of H_2PtCl_6 and $RuCl_3$ precursors, with the appropriate concentration, mixed with half its volume of isopropanol, to obtain a load of about 30 wt.% PtRu (1:1)/carbon black. The mixtures were reduced with an excess of formaldehyde, and dried at 110 °C during 12 h, to obtain catalysts labelled as IPR (PtRu/Vulcan), IPRN (PtRu/Vulcan-N) and IPRO (PtRu/Vulcan-O). A commercial catalyst 30 wt.% PtRu (1:1)/carbon (HiSPEC 5000, Johnson–Matthey) was used as reference.

2.2. Colloidal method [22]

The reaction was performed in water with aqueous solutions of reactants. The appropriate concentration of H_2PtCl_6 was reduced by adding a solution of $NaHSO_3$ to obtain a colourless soluble intermediate of platinum, which was then oxidized with H_2O_2 (30%, v/v). During the addition, the pH of the solution was adjusted to ca. 5 by adding Na_2CO_3. The appropriate amount of $RuCl_3$ solution was then added dropwise under continuous stirring. Adjustment of the pH to ca. 5 is again necessary. The required amount of carbon black was added to the colloidal solution under constant stirring. Hydrogen gas was bubbled through this admixture for 1 h, and the suspension was allowed to settle, filtered, repeatedly washed with hot water and then dried in an air oven at 110 °C for 16 h. The catalysts obtained (30 wt.% PtRu (1:1)/carbon black) was labelled as CPR (PtRu/Vulcan), CPRN (PtRu/Vulcan-N) and CPRO (PtRu/Vulcan-O).

Textural properties of the samples have been evaluated by N_2 adsorption–desorption isotherms of the samples recorded at the temperature of liquid N_2 with a Micromeritics ASAP 2000 apparatus. Samples were previously outgassed at 150 °C for 24 h. Specific areas were calculated by applying the BET method to portions of the isotherms within the $0.05 < P/P_0 < 0.30$ relative pressure range.

The pH was measured in an aqueous slurry containing 1 g of carbon black in 30 mL of water. This mixture was ultrasonically

dispersed during 2 min and stirred during 5 min. The pH was measured several times until a constant value was reached. The apparatus used was a pH-meter CG840 Schott Iberica.

The carbon elemental analysis was performed with an Elemental Analyzer CHNS-O Carlo Erba 1108 Instrument. The determination of the nature of the oxygen surface groups in the carbons was accomplished by temperature programmed desorption (TPD) analysis under Ar. Each sample was heated in an electric furnace at 10 °C/min from 30 to 950 °C under vacuum (2.5×10^{-5} mbar). The desorbed products were analysed by mass spectrometry using a Prisma TM QMS 200 of Balzers equipment coupled on line with a vacuum system. All figures containing ion current data from the TPD analysis are baseline corrected and normalized to the argon ion current measured during the thermal ramp and the initial sample weight.

Metal phases and crystalline particle size have been determined by using X-ray diffraction (XRD) measurements. X-ray diffraction powder patterns were obtained on a SEIFERT 3000P X-ray diffractometer, and using a Cu Kα-source. The powder diffractograms of the samples were recorded from 15° to 90° with a scanning rate of 0.04°/s.

Particle size and morphology as well as PtRu dispersion of the samples were evaluated from the transmission electron microscopy (TEM) images obtained in a JEOL 2000FX microscope operated with an accelerating voltage of 200 kV. Typically 10 mg of the sample were dispersed in acetone in an ultrasonic bath during 15 min. The sample was then placed in a Cu carbon grid where the liquid phase was evaporated.

The TXRF analysis was performed on a Seifert EXTRA-II spectrometer equipped with two X-ray fine focus lines, Mo and W anodes, and a Si(Li) detector with an active area of 80 mm^2 and a resolution of 157 eV at 5.9 keV (Mn Kα). The Pt/Ru atomic ratio was determined by using Pt Lα and Ru Lα emission lines in the XRF spectra after proper calibration with standard samples.

Photoelectron spectra (XPS) were obtained with a VG Escalab 200R spectrometer equipped with a hemispherical electron analyser (pass energy of 20 eV) and a Mg Kα ($h\nu$ = 1254.6 eV, 1 eV = 1.6302×10^{-19} J) X-ray source, powered at 120 W. The binding energies were calibrated relative to the C 1s peak from carbon contamination of the samples at 284.6 eV. For the analysis of the peaks a Shirley type background was used. Peaks were adjusted to a combination of Gaussian and Lorentzian functions using the XPSPeak 4.1 software.

The electrochemical measurements were carried out in a standard three electrode electrochemical cell at room temperature. The electronic equipment consisted of a Radiometer Analytical Model PGZ 301 potentiostat. The working electrode was prepared according to a modified method developed by Schmidt et al. [23]. A glassy carbon electrode 3.0 mm diameter (purchased from BAS) was used to this end. Previous to the deposition of the catalyst, the electrode was polished to a mirror ending with alumina and rinsed with triply distilled water. For the preparation of the ink 3.5 mg of the electrocatalysts were dispersed in water (1 mL) and Nafion (30 μL) in an ultrasonic bath during 45 min. Five microlitre of the ink were deposited onto the electrode and dried over an Ar flow for 30 min. All the potentials were referenced to the normal hydrogen electrode (NHE) and were measured versus a Hg/Hg_2SO_4. A Pt wire was used as the counter electrode. The electrolytes were purged with purified argon prior to each experiment. (CO_{ad}) was measured by CO stripping voltammetry in 0.5 M $HClO_4$ solution. Gaseous CO was purged into the cell for 12 min while maintaining a constant voltage of 0.02 V versus NHE. After CO removal (Ar purge during 30 min) the working electrode was subjected to a cyclic voltammetry step at a 10 mV/s scan rate, three consecutive cycles were recorded. The shape of the voltammogram obtained after CO oxidation is identical to those recorded under similar conditions previous to CO admission. The electrocatalytic activity of catalysts for methanol oxidation was studied in 0.5 M H_2SO_4 + 2 M CH_3OH.

3. Results

3.1. Support

The results of the BET surface area, pH measurements and elemental analyses are summarized in Table 1. The BET specific area of the supports decreased after nitric acid treatment, and it is similar to Vulcan with H_2O_2. The pH of the aqueous slurry of functionalited HNO_3 and H_2O_2 carbons decreases considerably, 2.6 and 3.3, respectively, compared to that Vulcan support, ca. 8.2.

The determination of the nature of the oxygen surface groups in the carbons was accomplished by TPD under Ar. Fig. 1 depicts both the CO (m/z = 28) and CO_2 (m/z = 44) desorption profiles of the supports. It may be observed that HNO_3 treatment generated an intense oxidation that resulted in large CO_2 and CO evolutions between 100–600 and 100–900 °C, respectively, compared with Vulcan-O. However, evolution of these gases from the untreated carbon Vulcan XC-72R is irrelevant in the scale used.

3.2. Catalysts

Table 2 shows the physicochemical parameters of the electrocatalysts based on analysis of TXRF, TGA, BET and TEM. Atomic ratio Pt:Ru (from TXRF) presents similar values (1:0.8) in all catalysts. TXRF and TGA measurements are used to calculate metal loading PtRu (wt.%). Values obtained by TGA when the support is completely calcinated, in flow of air, at 900 °C are also reported. Since XRD revealed that Pt^0 and RuO_2 are the only phases detected after catalyst firing in air, the Pt^0 + RuO_2 amounts are also included in Table 2. PtRu (wt.%) values are calculated with atomic ratio PtRu (TXRF) and Pt + RuO_2 (wt.%) values (TGA). BET specific area of the supports decreases with increasing metal loading.

Table 1
Characterization of carbon supports

Carbon black	BET (m^2/g)	pH	%C	%H	%N	%S	%O
Vulcan	203	8.2	98.0	0.1	0.1	0.5	0.3
Vulcan-O	200	3.3	96.5	0.1	0.0	0.6	1.1
Vulcan-N	159	2.6	90.0	0.3	0.2	0.5	6.9

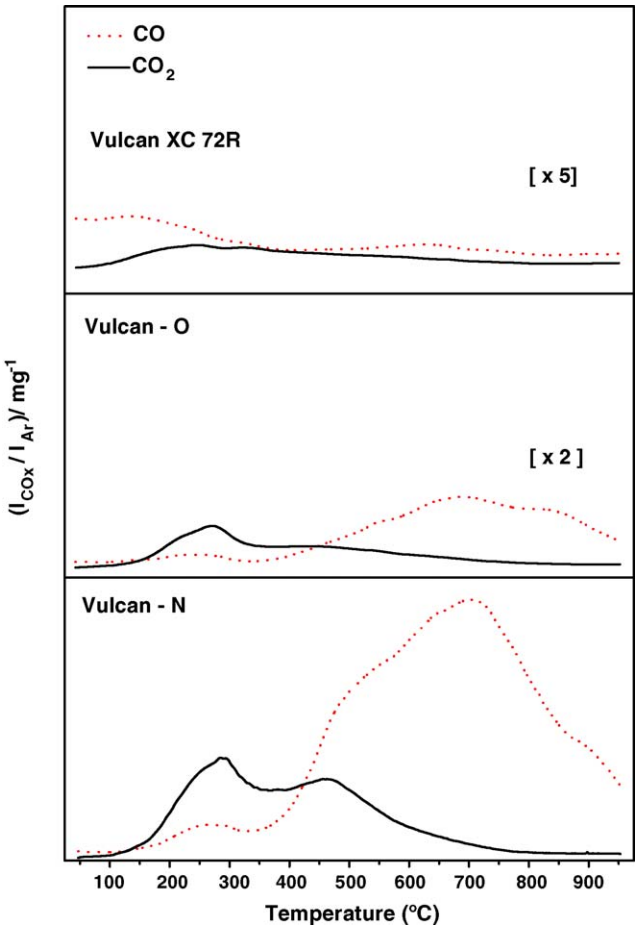

Fig. 1. TPD of Vulcan XC-72R, Vulcan-O and Vulcan-N.

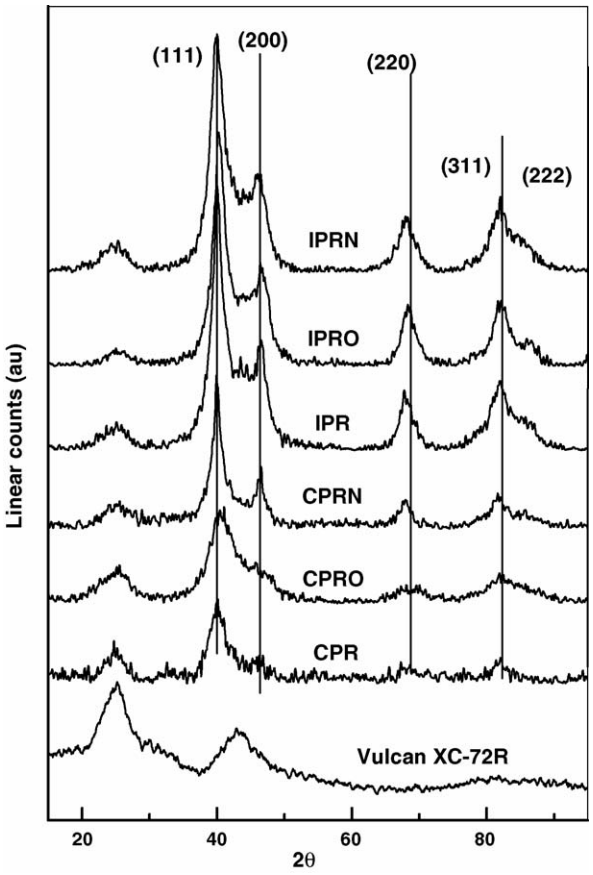

Fig. 2. X-ray diffractograms of catalysts.

X-ray diffractograms of Vulcan XC-72R substrate and of catalysts are shown in Fig. 2. All patterns of catalysts display diffraction lines of Pt fcc (JPCDS 40802). The electrocatalysts prepared by the impregnation method exhibit similar XRD patterns though peaks belonging to the (1 1 1), (2 0 0), (2 2 0), (3 1 1) and (2 2 2) planes are shifted to higher 2θ values with respect to the same reflections of the Pt fcc structure. Such a shift could account for the presence of a PtRu alloy in the catalyst [24]. The intensity of these lines decreases in CPRN catalyst, particularly in CPRO and CPR catalysts, due to the low crystallinity of the nanoparticles of Pt. Moreover, neither peaks of separate tetragonal RuO_2 nor of hexagonal close-packed (hpc) Ru phases are found. Vulcan XC-72R carbon and its functionalised derivatives (Vulcan-N and Vulcan-O) show the characteristic diffraction pattern of graphitic carbon.

Particle size and PtRu dispersion were evaluated from TEM and XRD (Table 2). The particle size distribution of catalysts CPR, CPRO and CPRN was found to lie between 2 and 4 nm while IPR, IPRO and IPRN catalysts show slightly larger particle sizes of 4–6 nm. Apparently, particle size depends on the preparation method. Oxidation of the support did lead to changes in the PtRu particle size in CPRN, which was 2 nm

Table 2
Physicochemical parameters of the electrocatalysts based on analysis of TXRF, TGA, BET and TEM and electroactive area (EAA)

Sample	Pt:Ru[a]	Pt + RuO_2[b]	PtRu[b]	BET (m^2/g)	Particle size (nm)		EAA[c] (m^2/g)	E_{pCO} (mV)
					TEM	DRX		
IPR	1:0.8	32	29	159	4.9	3.8	78.2	520
IPRO	1:0.8	33	30	157	6.0	3.7	61.4	500
IPRN	1:0.8	34	31	138	5.5	3.0	44.6	500
CPR	1:0.7	30	27	142	2.2	N.D.	80.4	462
CPRO	1:0.7	33	30	153	2.3	N.D.	124.3	450
CPRN	1:0.8	32	29	127	4.2	5.4	134.6	460

[a] Atomic ratio from TXRF.
[b] Wt.% from TGA.
[c] The electroactive area is calculated from the CO stripping experiment.

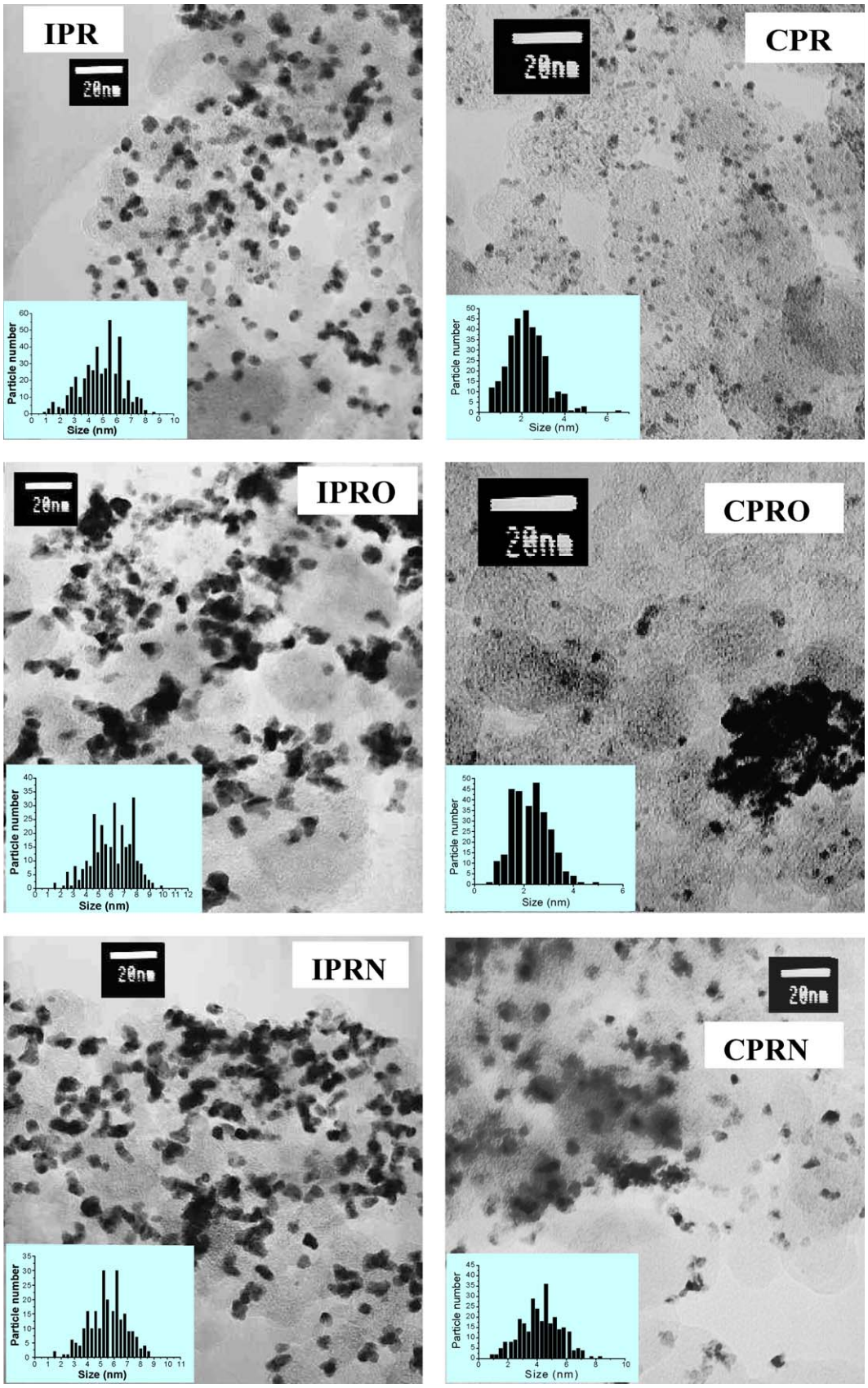

Fig. 3. TEM micrographs and particle size distribution of electrocatalysts.

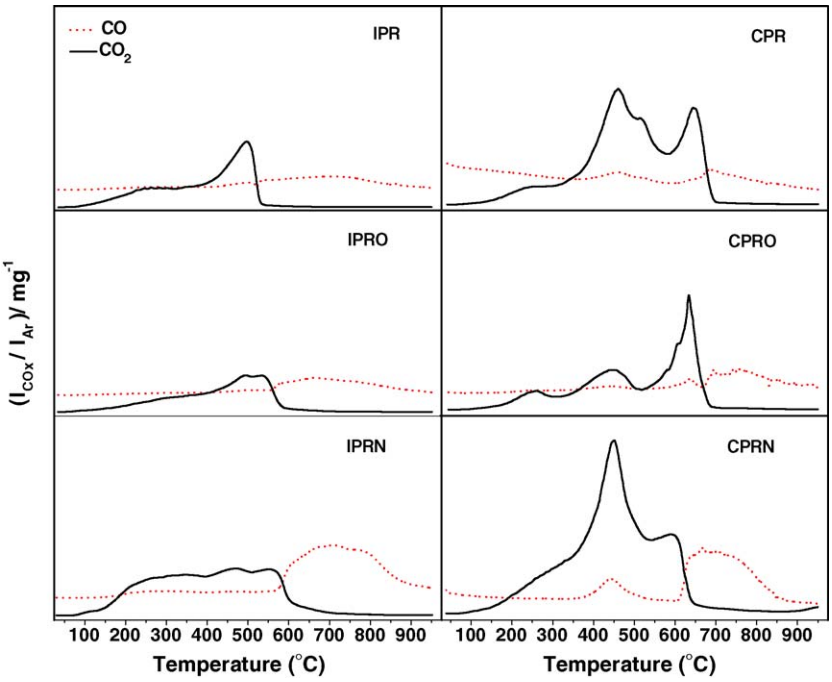

Fig. 4. CO (- - -) and CO_2 (—) desorption profiles of the different electrocatalysts.

higher than in CPR and CPRO. However, a better dispersion on the Vulcan XC-72R support than on Vulcan-O and Vulcan-N was observed. Agglomeration of small PtRu nanoparticles was found to occur on the CPRO, CPRN, IPRO and IPRN electrocatalysts as can be seen from Fig. 3, hence the slight discrepancy between particles sizes as determined from TEM and XRD techniques.

The TPD profiles of the different electrocatalysts are shown in Fig. 4. The intensity of CO and CO_2 desorptions are different depending on the preparation method. Besides, the relative intensity of the desorption peaks normalized to the total amount of the sample is depicted in Fig. 5. The catalysts prepared by the colloidal method led to larger CO_2 evolutions with a minor contribution of CO evolution. However, similar

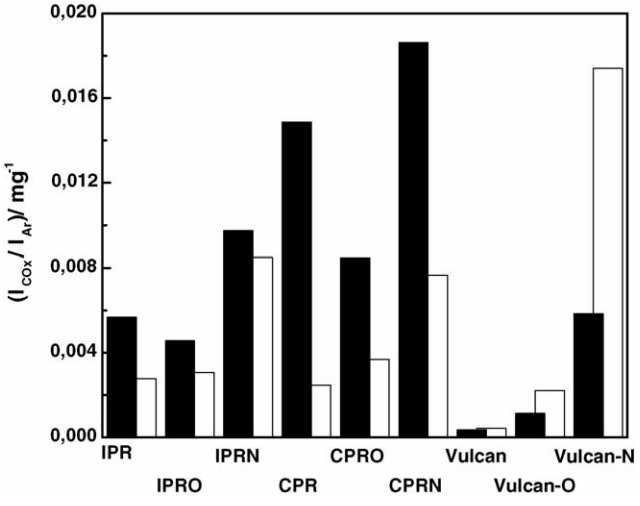

Fig. 5. Quantification (mg^{-1}) of desorbed amounts of CO (empty columns)and CO_2 (black columns).

CO_2 and CO evolution are observed on catalysts prepared by the impregnation method.

The nature of surface species of PtRu/carbon catalysts was investigated by XPS analysis. Both binding energies of core-levels and surface atomic ratios are given in Table 3.

The C 1s signal shows similar concentration of graphitic carbon (284.6 ± 0.2 eV) and oxidized (C–O) carbon species (285.6 ± 0.2 eV) in both series of catalysts. Thus after the synthesis of the electrocatalysts either by the impregnation or colloidal method, carbon black show similar amounts of carbon species. A low intensity broad band (FWHM > 4) at 288.6–289.8 eV is evident in the C 1s signal in all catalysts. Such band is due to a π–π^* transition characteristic of pure graphitic samples and it can be taken as an indirect measure of the graphitic character of carbon black [25]. The shape of this band is similar for all samples indicating that the graphite nature of the carbon is preserved. The O 1s core level spectra are shown in Fig. 6. The spectra of IPRN and IPRO samples derive three components whereas those of CPRO and CPRN catalysts show only two components. The lower BE peak (530.2–530.5 eV) can be related to PtO-like species, which are not observed in CPRO and CPRN catalysts. BE signal ca. 531.2–532.1 eV is attributed to –C=O groups, while at higher BE ca. 533.1–533.6 eV –C–OO groups (carboxylic) are found. CPRO and CPRN show a higher concentration (40%) of the more oxidized species (–C–OO) than the other catalysts. The O/C atomic ratio is higher for the Vulcan-N support, however similar O/C ratios are found for Vulcan-O and Vulcan XC-72R supports.

The Pt 4f signal doublet is derived from three pairs of Pt peaks except for CPRO with two pairs (Fig. 7a and b). The most intense Pt $4f_{7/2}$ component (71.4–71.8 eV) in all catalysts is attributed to metallic Pt. The Pt $4f_{7/2}$ component of the second doublet observed at 72.8–73.2 eV can be

Table 3
XPS results for the electrocatalysts

Sample	C 1s	O 1s	Pt $4f_{7/2}$	Ru $3p_{3/2}$	PtRu (wt.%)	O/C[a] (at.%)	Pt/C (at.%)	Ru/C (at.%)
IPR	284.4 (58)	530.2 (43)	71.6 (55)					
	285.6 (28)	531.7 (30)	73.2 (23)	462.7 (59)	28	0.031	0.019	0.013
	289.2 (14)	533.1 (27)	74.7 (22)	465.3 (41)				
IPRO	284.4 (54)	530.5 (42)	71.5 (56)					
	285.7 (31)	532.1 (31)	72.9 (22)	462.5 (59)	22	0.027	0.015	0.008
	288.9 (15)	533.5 (27)	74.4 (22)	465.1 (41)				
IPRN	284.4 (52)	530.5 (28)	71.4 (47)					
	285.7 (35)	532.0 (42)	72.8 (32)	462.4 (65)	26	0.059	0.019	0.010
	288.7 (13)	533.6 (30)	74.6 (21)	465.0 (35)				
CPR	284.5 (59)	530.5 (24)	71.8 (41)					
	285.6 (29)	531.4 (55)	72.8 (34)	463.2 (56)	17	0.037	0.010	0.007
	289.8 (12)	533.1 (21)	74.5 (24)	464.8 (44)				
CPRO	284.4 (60)							
	285.4 (24)	531.2 (61)	71.6 (56)	462.3 (100)	6	0.036	0.003	0.001
	289.4 (15)	533.1 (39)	72.9 (44)					
CPRN	284.5 (57)		71.7 (46)					
	285.3 (29)	531.4 (60)	73.0 (41)	463.3 (59)	11	0.119	0.005	0.008
	288.6 (15)	533.4 (40)	74.9 (13)	465.0 (41)				

[a] The contribution of the oxygen component of PtO species is neglected for the calculation of the oxygen atomic ratios.

assigned to Pt^{2+} species in PtO and $Pt(OH)_2$-like species [26]. An additional set of Pt peaks whose major Pt $4f_{7/2}$ component appears at even higher BEs (74.4–74.9 eV) corresponds to a higher oxidation state (Pt^{4+}), which is absent in CPRO and shows a weaker intensity in CPRN. The Ru $3p_{3/2}$ signal derives of two components with BEs of 462.3–463.3 and 464.8–465.3 eV, except for CPRO, which only shows one component (462.3 eV). These peaks could be attributed to RuO_2 and RuO_3 species, respectively [26]. Yet, the width of ca. 3 eV of the main peak suggests that this component could derive from the contributions of more than one species with similar BEs [27].

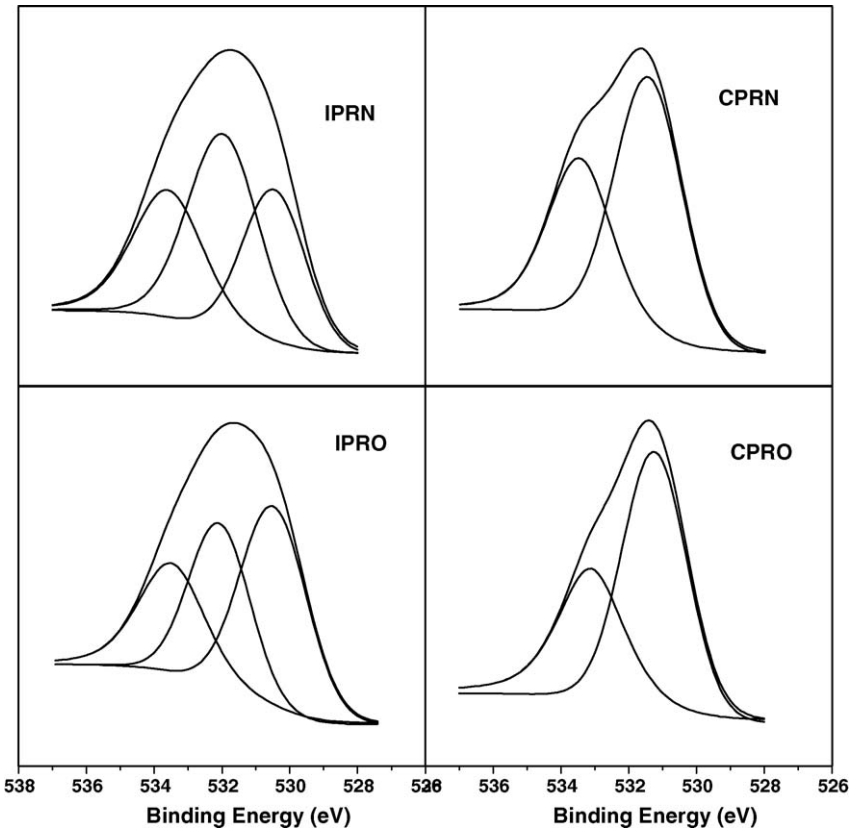

Fig. 6. XPS spectra of O 1s of IPRN, IPRO, CPRN and CPRO electrocatalysts.

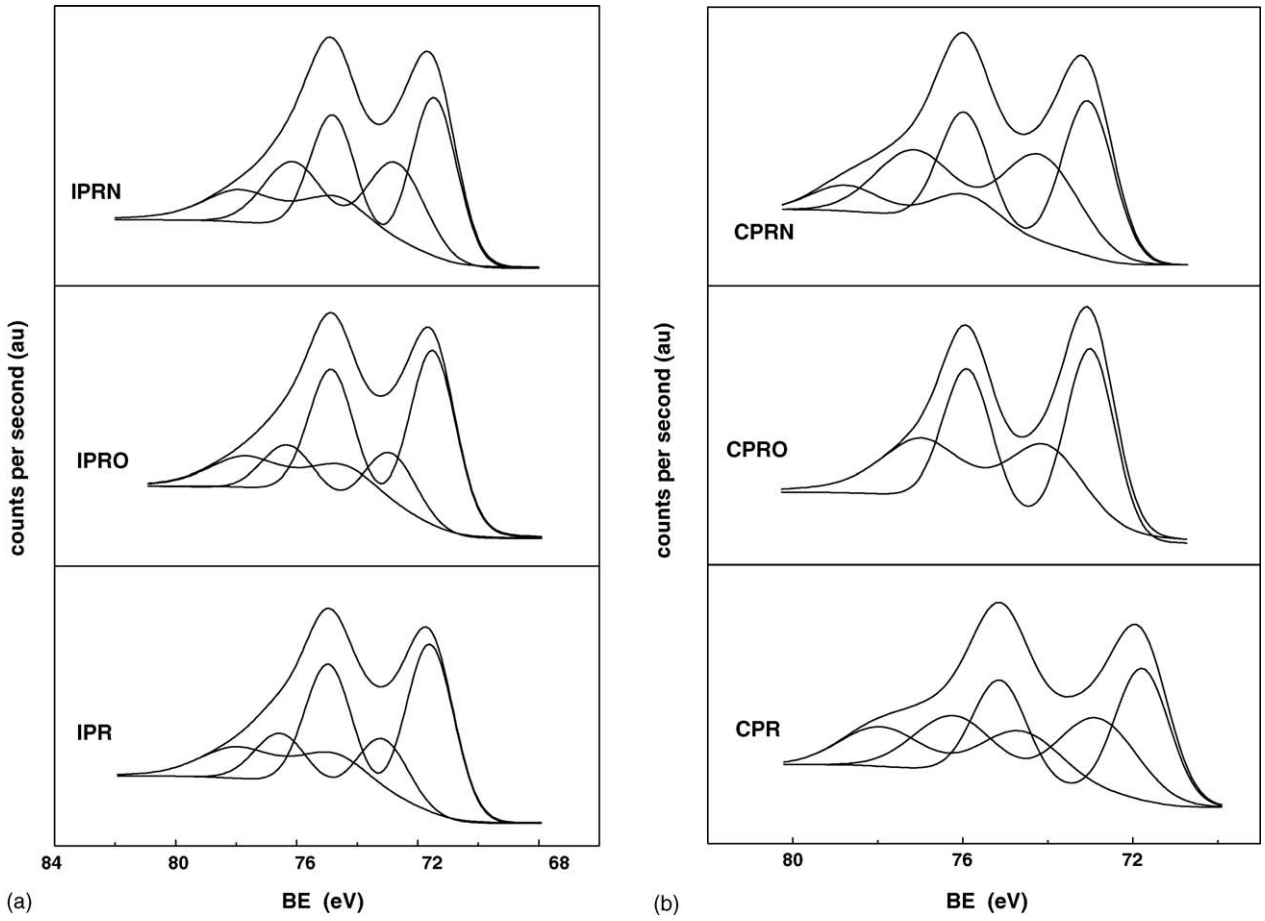

Fig. 7. XPS spectra of Pt 4f of electrocatalysts: (a) impregnation series and (b) colloidal series.

Quantitative evaluation of PtRu content by XPS revealed that in the samples prepared by the colloidal method the surface concentration of the metals is much lower than in the bulk material (ca. 30%), particularly in CPRO (6 wt.%) and CPRN (11 wt.%). However, similar surface concentration of metals is observed for IPR (28 wt.%), IPRO (22 wt.%) and IPRN (26 wt.%), which are closer to expected values.

3.3. Electrochemical characterization

Prior to the CH_3OH oxidation studies, the catalysts were characterized by CO_{ads} stripping voltammetry. The stripping technique provides information about the facility of the material towards CO oxidation, which can be directly correlated with the nature of the material. In addition, the extent of the CO oxidation process gives information about surface area of the metal that is accessible to the reactants [28,29]. Fig. 8 shows the CO_{ads} stripping voltammograms of the different samples recorded at room temperature. The CPR, CPRO, CPRN and electrocatalysts show similar behaviour for the CO_{ads} stripping peak ($E_p = \sim 0.45$ V), similar to that of the reference catalysts $E_{pCO} = 0.45$. The potential position of the maximum CO_{ads} stripping peak (E_{pCO}) in the IPR, IPRO and IPRN catalysts is shifted towards more positive potential ($E_p = \sim 0.50$ V). E_{pCO} values of the different samples are collected in Table 2. The Pt + Ru surface area values estimated using the CO_{ads} method (Table 2) indicate that the electroactive Pt + Ru surface area for catalysts prepared by the colloidal method, specifically CPRO and CPRN, is much higher than for the catalysts prepared by the impregnation method.

Methanol electrooxidation was evaluated by chronoamperometry, the results being plotted in Fig. 9. The response, as current densities normalized to the metal area determined from the CO stripping analysis, increased in the order: CPR < IPR ∼ IPRO < IPRN < PtRu (J&M) ∼ CPRN < CPRO. The electrocatalysts prepared by the colloidal method after pretreating the carbon black substrate with HNO_3 and, especially with H_2O_2, displayed higher activity per area unit of metal than the Johnson and Mattey reference.

4. Discussion

The elemental analysis results (Table 1), the TPD profiles (Fig. 1) and the decrease in pH (Table 1) indicate the presence of oxygen species after processing the carbon substrate with H_2O_2 and more specifically with HNO_3. Oxidation treatment of carbonaceous materials develops a great variety of surface oxygen complexes [12,18]. These O-species are classified as acidic, basic or neutral, depending on the pH of the carbon aqueous slurry. In the catalysts of this work, the acidic surface

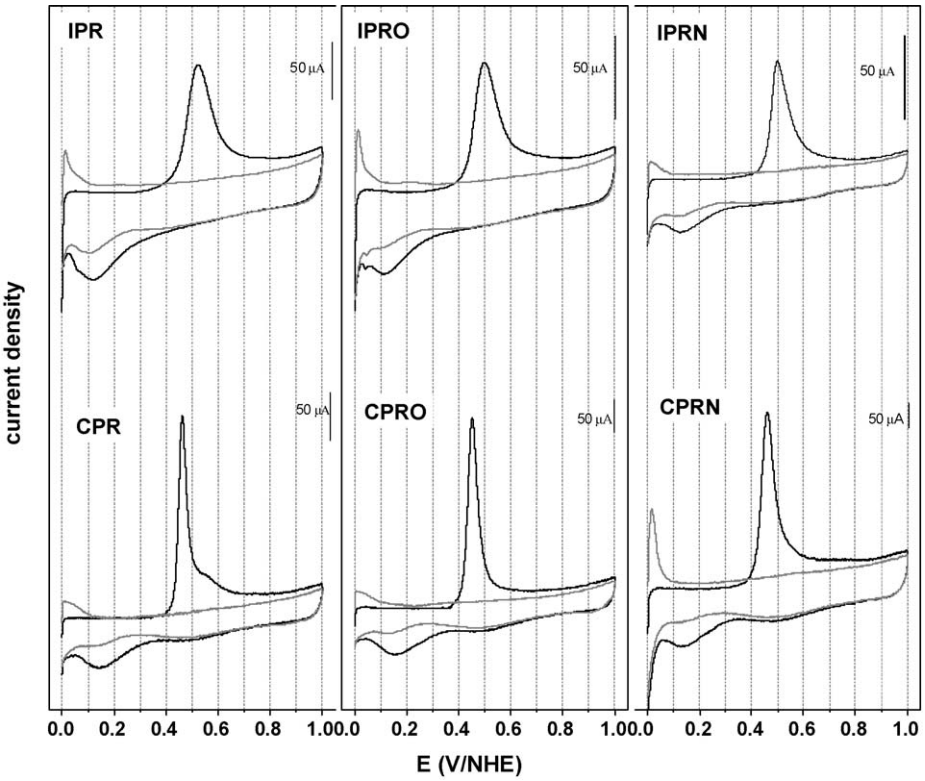

Fig. 8. CO_{ads} stripping voltammograms of the electrocatalysts. In the first cycle (black) the CO oxidation is observed. In the second cycle (grey) the hydrogen features are observed.

properties are due to the presence of acidic surface groups. TPD analysis has been conducted at different temperatures with the aim to identify surface functional groups on the carbon surface. Surface oxygen groups decomposed upon heating under the inert atmosphere, the stronger acidic groups (carboxylic groups and their derivatives, such as lactones and anhydrides) evolved CO_2, and the weaker acidic groups (quinones, hydroquinones, ethers, carbonyls and phenols) evolved CO [18]. Thus, TPD profiles indicate that pretreatment of carbon substrate with HNO_3 and H_2O_2 develop both types of acid groups, mostly weak acid groups that decompose at higher temperatures than the stronger ones (Fig. 1).

The relationship between CO_2 and CO desorption profiles of the electrocatalysts (Fig. 5) depends on the preparation method. The amount of strong acid groups evaluated by CO_2 desorption is higher in the catalysts prepared by the colloidal method. These results could be correlated with XPS data, which reveal an increase in the amount of the more oxidized surface species (–C–OO), and specifically in CPRO and CPRN samples.

The role exerted by the oxygen concentration on the surface of the carbon on the Pt catalyst dispersion has been studied by other authors [17,18,30,31]. They observed a decrease in the platinum dispersion with an increase in the fraction of oxygen-containing surface functionalities of the carbon support. Indeed, our previous results demonstrated a similar trend between the amount of surface oxygen species and dispersion degree of platinum metal [32,33]. The same effect is observed upon incorporation of ruthenium on functionalited carbon black. Therefore, there is an important effect on the dispersion of the crystallites of noble metals upon treatment of carbon substrate with H_2O_2 and HNO_3. Moreover, the particle size distribution depends on the preparation method. Larger crystallite sizes were observed in catalysts prepared by the impregnation method (5–6 nm), however the particle size decreases when they are prepared by colloidal method (2–4 nm).

Both the chemical treatment of Vulcan XC-72R substrate and the preparation method affect to a significant extent the activity of the samples. Electrocatalysts derived from the colloidal method show similar behaviour in the CO_{ads} stripping process than the commercial catalyst. Furthermore, CPRN and CPRO samples display the best performance in methanol electrooxidation. These results can be rationalized by assuming that most of the PtRu particles are within the pores, and cannot be detected by XPS, resulting in a low surface concentration. However, as they are accessible to the reactants, as catalysts these samples are endowed with a superior activity. In good agreement with the particle size determined by XRD and TEM, the electrochemical characterization indicates that the number of active metallic surface centres is higher in CPRN and CPRO catalysts.

One of the reasons that can be put forward to explain the lesser activity of the catalysts synthesized by the impregnation method is their particle size, being 2–3 nm larger than that of the catalysts prepared by the colloidal methodology. Another reason could be related to the nature of PtRu species. Analyses of the catalysts by photoelectron spectroscopy are conclusive on the presence of Pt^0, Pt^{2+} and Pt^{4+} species in most of the

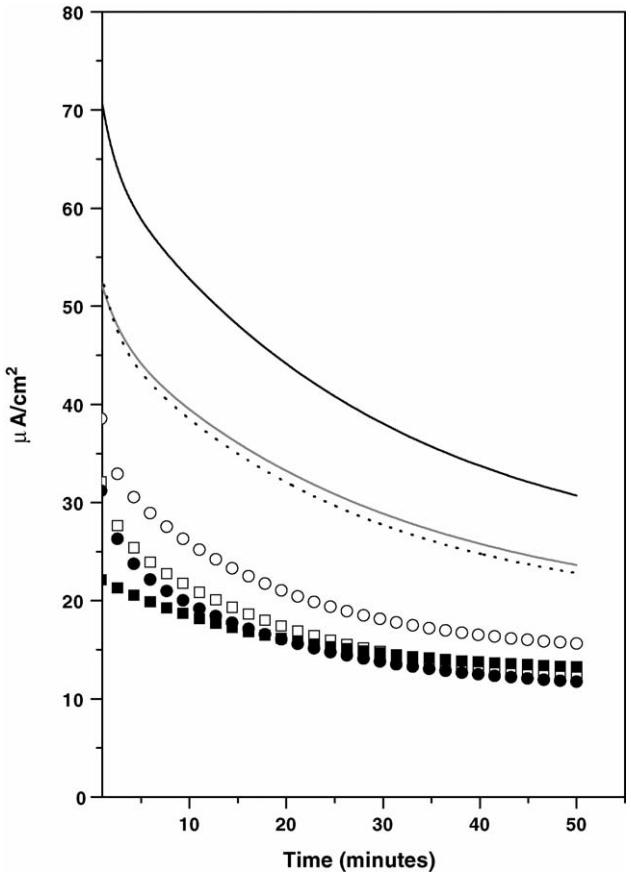

Fig. 9. *j*/*t* response recorded at 500 mV (RHE) in MeOH (2 M) in H_2SO_4 (0.5 M). Current density is normalized to the electroactive Pt + Ru area estimated from CO_{ads} stripping voltammograms. (–) CPRO; (▬) CPRN; (. . .) commercial; (○) IPRN; (□) CPR; (●) IPRO; (■) IPR.

catalysts particularly in those prepared by the impregnation method. However, catalysts obtained by the colloidal method supported on functionalited carbon, CPRN and CPRO, exhibit less or even no Pt^{4+} species. Therefore, an important effect due to preparation method is the modification of the structure of Pt. Aricò et al. [34] observed an increase of oxidized Pt species in a PtRu/carbon catalyst with respect to the Pt/carbon sample, which would explain the development of metal–support interaction due to the change of catalyst preparation conditions. Simultaneously, acid groups on the surface of carbon could affect the oxidation sate of platinum, which is less oxidized on Vulcan-N and especially on Vulcan-O than over the Vulcan XC-72R support, indicating a high oxidation-resistance over acidic support than on the untreated one [35], but always depending on the preparation method.

It was previously observed [27,34] that the close association of Ru with Pt in a carbon-supported bimetallic (PtRu) catalyst produced a significant shift of the Ru 3p signal to a higher BE value (ca. 1 eV) compared to a Ru/carbon catalyst obtained in a similar way. This effect was attributed to an electron transfer involving Ru and Pt within the alloy. Since the electronegativity values of these elements are 2.20 and 2.28, respectively, Pt atoms produce an electron withdrawing effect from the neighbouring Ru atoms, influencing the polarization or the Pt–Ru bond in the alloy [27]. In light of these arguments, it could be suggested that the main component in the Ru 3p signal derives from both contributions of Ru, i.e. the alloy and Ru^{4+} species. While many results in the field of electrocatalysts allowed getting a detailed knowledge of electrode processes and mechanisms, comparatively little is known about the structure and nanomorphology of the real catalysts. Studies of several PtRu catalysts [36,37] show a common feature: they are more active, even if they were incompletely alloyed and contained significant amounts of oxide phases of ruthenium. Thus, there is a significant promotion effect for oxidation caused by the mere presence of ruthenium without the need of substantial alloy formation.

The higher activity in CPRO and CPRN catalysts could be rationalized by assuming two effects. The first one is the preparation method that mainly affects the structure of the PtRu nanoparticles. Colloidal method renders smaller particles, which are located into the mesoporous structure of the carbon support. The second one is due to the functionalisation of carbon black that will increase the concentration of oxidized groups on its surface, facilitating the accessibility of the reactants (methanol and CO) to the electroactive surface and participate in the oxidation of the adsorbed intermediate species formed in methanol dissociation.

5. Conclusions

There are significant differences in the physicochemical properties of the electrocatalysts due to the preparation method: (a) the impregnation method develops particle size of 2–4 nm higher than the colloidal method; (b) quantitative evaluation of PtRu content (XPS) reveal that the surface concentration of the metals is much lower on catalysts obtained by the colloidal method (11–17%) than those obtained by the impregnation method (22–28%); (c) large amounts of strong acid groups (TPD) are developed in the catalysts prepared by the colloidal method.

The main effect of the CPRO, CPRN, IPRO and IPRN catalysts due to the treatment of the carbon is the formation of small PtRu nanoparticles agglomeration. However, the electrochemical activity between CPRO, CPRN and IPRO, IPRN is significantly different, where the performance of catalyst obtained by the colloidal method is considerably higher. Therefore, the different structure of PtRu nanoparticles due to preparation method, and the increase of oxidized groups' concentration, particularly strong acid groups in CPRO and CPRN, could explain a better performance of these catalysts.

Acknowledgements

Financial support from MCyT, Spain, under Project MAT2001-2215-C03-01 is acknowledged. The authors would like to thank Dr. E. Pastor and Dr. J.L. Rodriguez at University of La Laguna (ULL), Spain, for their support. Thanks are also due to the Fuel Cell Network (CSIC) for institutional assistance. M.V. Martínez-Huerta acknowledges the Juan de la Cierva Program of the Ministry of Science and Technology of

Spain for financial support. S. Rojas acknowledges the Ramon y Cajal Program of the Ministry of Science and Technology of Spain for financial support. J.L.G. de la Fuente acknowledges to the I3P program (CSIC) for financial support.

References

[1] T. Iwasita, in: W. Vielstich, et al. (Eds.), Handbook of Fuel Cells, vol. 2, Wiley, Chichester, UK, 2003, p. 603.
[2] J. Müller, G. Frank, K. Colbow, D. Wilkinson, in: W. Vielstich, et al. (Eds.), Handbook of Fuel Cells, vol. 4, Wiley, Chichester, UK, 2003, p. 847.
[3] A. Hamnett, Catal. Today 38 (1997) 445.
[4] E.A. Batista, G.R.P. Malpass, A.J. Motheo, T. Iwasita, J. Electroanal. Chem. 571 (2004) 273.
[5] E.A. Bagotski, Y.B. Vassiliev, O.A. Khazova, J. Electroanal. Chem. 81 (1977) 229.
[6] A.S. Aricò, R. Srinivasan, V. Antonucci, Fuel Cells 1 (2001) 133.
[7] M. Watanabe, S. Motoo, J. Electroanal. Chem. 60 (1975) 267.
[8] T. Frelink, W. Visscher, J.A.R. van Veen, Surf. Sci. 335 (1995) 353.
[9] E. Auer, A. Freund, J. Piestch, T. Tacke, Appl. Catal. A: Gen. 173 (1998) 259.
[10] D. Pantea, H. Darmstadt, S. Kaliaguine, C. Roy, Appl. Surf. Sci. 217 (2003) 181.
[11] Y. Otake, R.G. Jenkins, Carbon 31 (1993) 109.
[12] H.P. Boehm, Carbon 32 (1994) 759.
[13] J.S. Noh, J.A. Schwarz, Carbon 28 (1990) 675.
[14] S.R. de Miguel, J.C. Heinen, A.A. Castro, O.A. Scelza, React. Kinet. Catal. Lett. 40 (1989) 331.
[15] K.M. Colbow, J. Zhang, D.P. Wilkinson, US Patent 6,153,323 (2000).
[16] G.C. Torres, E.L. Jablonski, G.T. Baronetti, A.A. Castro, S.R. de Miguel, O.A. Scelza, M.D. Blanco, M.A. Peña Jiménez, J.L.G. Fierro, Appl. Catal. A: Gen. 161 (1997) 213.
[17] P.L. Antonucci, V. Alderuci, N. Giordano, D.L. Cocke, H. Kim, J. Appl. Electrochem. 24 (1994) 58.
[18] M.C. Román-Martínez, D. Cazorla-Amorós, A. Linares-Solano, C.S.-M. de Lecea, H. Yamashita, M. Anpo, Carbon 33 (1995) 3.
[19] Y. Verde, G. Alonso, V. Ramos, H. Zhang, A.J. Jacobson, A. Keer, Appl. Catal. A: Gen. 277 (2004) 201.
[20] V.M. Jovanovic, S. Terzic, A.V. Tripkovic, K.Dj. Popovic, J.D. Lovic, Electrochem. Commun. 6 (2004) 1254.
[21] Z.B. Wang, G.P. Yin, P.F. Shi, Carbon 44 (2006) 133.
[22] M. Watanabe, M. Uchida, S. Motoo, J. Electroanal. Chem. 229 (1987) 395.
[23] T.J. Schmidt, M. Noeske, H.A. Gasteiger, R.J. Behm, P. Britz, H. Bönnemann, J. Electrochem. Soc. 145 (1998) 925.
[24] D. Chu, S. Gilman, J. Electrochem. Soc. 143 (1996) 1685.
[25] H. Estrade-Szwarckopf, Carbon 42 (2004) 1713.
[26] D. Briggs, M.P. Seah, in: D. Briggs, M.P. Seah (Eds.), Practical Surface Analysis by Auger and X-Ray Photoelectron Spectroscopy, Wiley, New York, 1990.
[27] J.B. Goodenough, R. Manoharan, A. Shukla, K.V. Ramesh, Chem. Mater. 1 (1989) 391.
[28] N.M. Markovic, P.N. Ross, CATTECH 4 (2000) 110.
[29] J.C. Davies, B.E. Hayden, D.J. Pegg, M.E. Rendall, Surf. Sci. 496 (2002) 110.
[30] K.L. Yeung, E.E. Wolf, J. Catal. 135 (1992) 13.
[31] F. Coloma, A. Sepúlveda-Escribano, J.L.G. Fierro, F. Rodríguez-Reinoso, Langmuir 10 (1994) 750.
[32] J.L.G. de la Fuente, S. Rojas, M.V. Martínez-Huerta, P. Terreros, M.A. Peña, J.L.G. Fierro, Carbon 44 (2006) 1919.
[33] J.L.G. de la Fuente, M.V. Martínez-Huerta, S. Rojas, P. Terreros, J.L.G. Fierro, M.A. Peña, Carbon 43 (2005) 3002.
[34] A.S. Aricò, P. Creti, H. Kim, R. Mantegna, N. Giordano, V. Antonucci, J. Electrochem. Soc. 143 (1996) 3950.
[35] Y. Yazawa, H. Yoshida, T. Hattori, Appl. Catal. A: Gen. 237 (2002) 139.
[36] C. Roth, A.J. Papworth, I. Hussain, R.J. Nichols, D.J. Schiffrin, J. Electroanal. Chem. 581 (2005) 79.
[37] J.W. Long, R.M. Stroud, K.E. Swider-Lyons, R. Rolison, J. Phys. Chem. B 104 (2000) 9772.